

TWO EXAMPLES OF USING ERS-2 SAR INTERFEROMETRY IN GREECE. STUDY OF THE SEPTEMBER 7, 1999 ATHENS EARTHQUAKE AND THE NISYROS VOLCANO ACTIVITY

**C. Kontoes ⁽¹⁾, O. Sykioti ⁽¹⁾, P. Elias ⁽¹⁾
P. Briole ⁽²⁾, D. Remy ⁽²⁾
M. Sachpazi ⁽³⁾
G. Veis ⁽⁴⁾, I. Kotsis ⁽⁴⁾**

⁽¹⁾ National Observatory of Athens, Institute for Space Applications and Remote Sensing, Metaxa & Vas. Pavlou, 152

36, Palea Penteli, Athens, Hellas, Email: kontoes@creator.space.noa.gr

⁽²⁾ UMR-CNRS 7580, Département de Sismologie, Institut de Physique du Globe de Paris, 4 Place Jussieu,

75005 Paris, France. Email: briole@ipgp.jussieu.fr

⁽³⁾ National Observatory of Athens, Institute for Geodynamics, Lofos Nimfon, 118 10 Athens, Hellas,

Email: m.sachp@egelados.gein.noa.gr

⁽⁴⁾ National Technical University of Athens, Department of Surveying Engineering, 15780, Athens, Hellas,

Email: inveis@otenet.gr

ABSTRACT

Using combinations of adequately selected ERS-2 SAR images, the co-seismic deformation field associated with the Athens earthquake was analyzed. The observed fringes indicate a minimum of 56mm change in slant range direction. To assess the location and geometry of the seismic fault and the amplitude of the slip, a simple dislocation model in elastic half-space was assumed. The model suggests ~300 mm slip on an 18 km long blind fault composed of two pieces. The intersection of the fault plane with the Earth surface is located in the Fili mountain with a ~N120° orientation.

Interferometric analysis of ERS-2 SAR images from Nisyros volcano show that significant crust uplift of the order of 140mm has occurred during the years 1995-1997. The years 1997-2000 an opposite sign crust deformation has been observed as being the result of a deflation procedure. The first results on the study suggest that the presently active part of the Nisyros caldera appears to be much smaller than the known geological one with the existence of a magma chamber at the NW coast of Nisyros island. The inflation and deflation of this chamber is responsible for the unrest episodes recorded during the last years.

INTRODUCTION

Interferometric analysis of SAR images has demonstrated potential to monitor, measure and map surface deformations associated with earthquakes and other geophysical phenomena [11], [23], [15]. In Greece it has been used in the past for the study of the $M_w=6.6$ May 13, 1995, Kozani, and $M_w=6.1$ June 15, 1995, Aigion earthquakes in Greece [14], [2]. This technique was used by Massonnet [12] to measure the deflation induced by the activation of Etna volcano in the period from May 17, 1992 to October 24, 1993. Also the deformation field associated with the 1997 eruption of Okmok volcano in Alaska [9] and the Campi Flegrei caldera activation near Pozzuoli harbour [1], have been studied by constructing interferograms from the phase difference of SAR images recorded by ERS-2 satellite.

Interferograms are the result of the difference in phase values recorded by two SAR images. The phase differences correspond to changes in the round trip path length of the radar wave to the ground target. These changes are attributed to topography, geometry of satellite orbital trajectories, tropospheric and ionospheric perturbations and certainly to ground deformations due to geophysical phenomena. Given that atmospheric perturbations are negligible compared to other artifacts (e.g Digital Elevation Model (DEM) errors) and that the orbit geometry is perfectly known or adequately corrected, the isolation of the surface deformation component in an interferogram is possible only if the topography has been removed from it. In both studies described in this paper, the topography was removed by applying the "two-pass interferometry or DEM Elimination" method. With this approach a synthetic fringe pattern derived from the DEM of the study area is subtracted from the interference pattern resulted by the two SAR images [13]. The remaining changes in the satellite-to-ground ranges are represented by fringes. Each fringe corresponds to a movement along the viewing axis of the satellite by half a wavelength, which equals 28 mm for the C band microwave radar used by ERS-2 satellite.

In this paper we describe two studies for which SAR interferometry has provided significant information for two cases of geophysical activity in Greece. The one aims to identify the seismogenic fault and its parameters associated with the September 7, 1999 Athens earthquake. The second study, which is still under investigation, deals with the monitoring of the volcanic activity in Nisyros island during the recent long lasting episode of unrest spanning the years 1995-2000.

Case Study 1: The September 7, 1999 Athens Earthquake

Mapping and Modeling the Surface Deformation

On September 7, 1999 at 11^h 56^m 50^s UT a magnitude $M_w=5.9$ earthquake struck the city of Athens. Its epicenter was located at 38.1°N; 23.56°E which is about 20km NNW from the Athens center. The earthquake was a rather unexpected event, it was strongly felt by the Athenian population, caused many damages and made several buildings collapse killing 143 people. Scientists believe that its occurrence will change the perception of seismic hazard studies for the years to come, since greater Athens has been considered for many years as a region of low seismicity.

The earthquake has occurred between several normal faults dipping northward or southward clearly expressed on the seismotectonic map (Fig. 1). Two faults which are easily identified trending ESE-WNW, dominate the neotectonic behavior of this region. These are the 120°N striking Aspropyrgos fault (F1) and the 110-130°N striking Fili fault (F2) (Fig.1) [17]. The Aspropyrgos fault borders the Thriassion depression to the north, is 10 km long and its extremities are defined by the coordinates 28.13°N; 23.13°E, and 38.08°N; 23.66°E. The Fili fault lies ~5km to the north and is about 8km long. Both faults uplift Mesozoic limestone in their footwall blocks. Faults within limestone bedrock can usually be identified from exposed fault planes along the tops of the scree cones, fairly steep dissected ridges and longitudinal drainage patterns. However, field investigation [N.N. Ambraseys, internal field report] confirms that this is not apparent along the Aspropyrgos fault where a significant amount of erosion of the resistant limestone footwall exists, suggesting insufficient tectonic activity for keeping the subsiding hanging wall block in a depositional environment. On the other hand the Fili fault is a short length feature with no distinct break in slope, a fairly dissected footwall ridge and a discontinuous hanging wall basin.

The location of these two faults made scientists to believe that they could have been associated with the earthquake event. However, intensive field checks conducted immediately after the earthquake did not show any direct evidence of reactivation of any of the faults. Apart from occasional rock falls from south-facing steep slopes related mainly to

sliding, no significant co-seismic surface faulting is observed [N.N. Ambraseys, internal field report]. To understand the seismic process in the area, several operations have been initiated to record the aftershock activity by deploying locally seismograph arrays. At the same time a parallel operation using radar interferometry was initiated to map the co-seismic deformation field associated with the earthquake and draw conclusions on the seismogenic fault and its parameters.

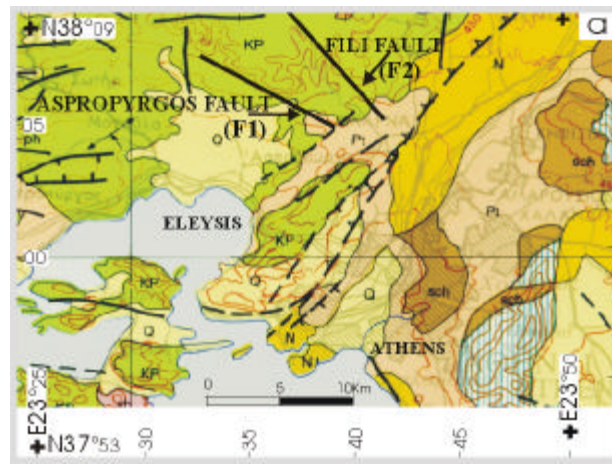


Fig.1 Seismotectonic map of Athens with seismogeological elements. The Fili (F2) and Aspropyrgos (F1) faults are indicated

Several ERS-2 SAR images were collected for interferometric calculations. They are spanning the period between December 1995 to October 1999. The images belong to the descending pass of the ERS-2 system, where the satellite travels approximately from north to south looking westwards and inclined 23.5° from the vertical. The selection of the interferometric pairs to process was based on their sensitivity to the topography, expressed by the altitude of ambiguity h_a . For the elimination of the topography, a synthetic fringe pattern produced by using a ± 10 m-accuracy DEM was subtracted from the interference pattern resulted by the two SAR images. Given that the h_a values for the four co-seismic interferograms range between 50 m to 133 m, it is expected that the topographic artifacts in the calculated interferograms would be between 5.6 mm (0.2 phase cycles) and 2.1 mm (0.075 phase cycles) respectively. Fig. 2 in the following illustrates the time spanning of the usable interferometric pairs and their corresponding h_a values. The interferograms, calculated using the DIAPASON (CNES) software.

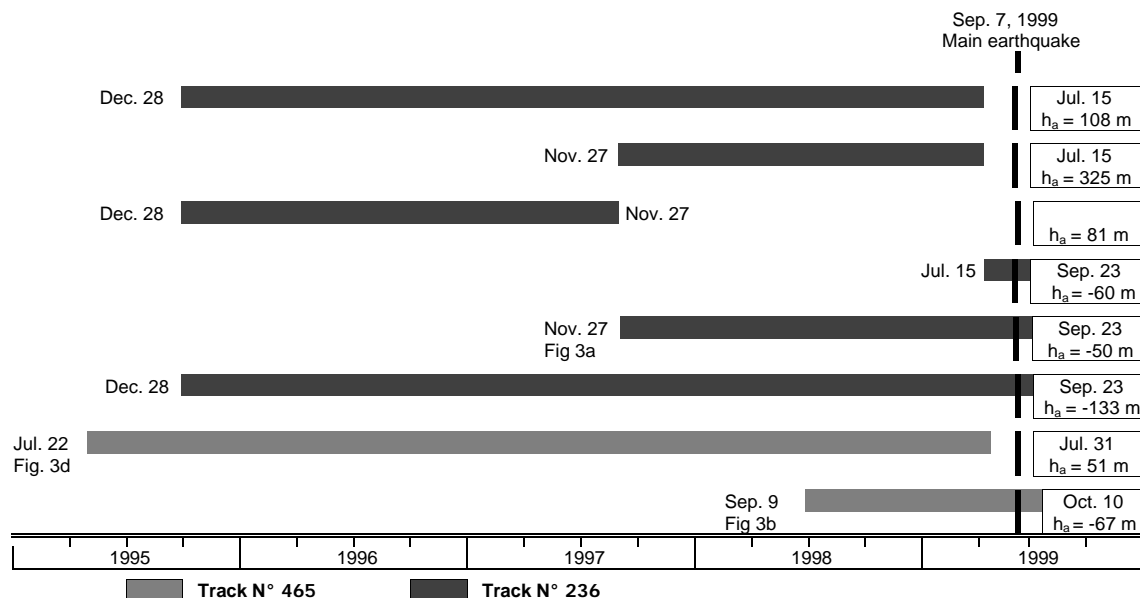


Fig 2. Bar chart showing the time spanning of the interferometric pairs. The numbers on the right-hand side of each bar indicate the ending date and the altitude of ambiguity h_a . The values at the left-hand side indicate the starting date and the figure codes of the interferograms.

The calculated co-seismic interferograms show that the earthquake caused surface deformations, which appear with at least two concentric, but not symmetric fringes, centered at 38.10°N; 23.60°E. This point is located in a distance of less than 3 km away from the main epicenter (38.10°N, 23.56°E). The resulted fringes indicate 56 mm of change in slant range direction. Fig. 3a and 3b show two co-seismic interferograms composed from images spanning the periods [Nov. 27, 1997 to Sep. 23, 1999] and [Sep. 19, 1998 to Oct. 9, 1999]. The study of the interferograms shows that the observed fringes are rather constant in shape, position and magnitude and that they are the result of a co-seismic surface deformation. The number and concentric pattern remain the same in all interferograms, although they have different h_a values (133m, 67m, and 50m) and they are issued from images acquired from adjacent tracks, namely 236 (Fig. 3a) and 465 (Fig. 3b). In addition all the pre-seismic interferograms do not show any fringes (Fig. 3c).

The resulted co-seismic fringes were used to sample slant range displacements at 134 discrete points along them. The sampled data were input to an inversion model, assuming dislocations of rectangular planes in an homogeneous elastic half-space [16]. Table 1 shows the variables used in the model. The inverse algorithm is that developed by *Briole* [3] using the least squares approach proposed by *Tarantola and Valette* [20]. The inversion program was run first assuming a single rectangular fault, but the model could not correctly fit the asymmetry at the eastern end of the fringe pattern. Therefore a secondary fault was added in order to fit better the observed fringes.

Two models were examined. In model 1, all parameters were kept free except for the strike slip that was forced to zero (pure normal faulting). In model 2, the strike and dip angles were fixed at 116° and 54° respectively, so as to conform to the focal mechanism of the earthquake [21], [18] and with the orientation of the known tectonic structures [17]. The results showed that both models fit the observed fringes well (rms error for data fit was 4 mm for model 1 (0.14 fringes) and 5.5 mm (0.19 fringes) for model 2). However, the suggested by model 1 strike (100°) and dip (43°) angles were not consistent with the preliminary fault-plane solutions indicating strike directions and dip angles in the ranges of 113°-119°N and 52°-56° respectively [21], [18]. As a consequence the fault parameters obtained by model 2 have been kept. Table 2 gives the fault parameters obtained by model 2. According to the model most of the observed surface deformations are due to a dip-slip along the main fault segment. The secondary fault segment, which is responsible for the observed asymmetry of the deformation field, corresponds to a shallower rupture. The two fault segments intersect the Earth surface at points: 38.18°N; 23.55°E - 38.14°N; 23.66°E (main fault) and 38.16°N; 23.66°E - 38.12°N; 23.75°E (secondary fault). These two traces lie at 5 km and 7.5 km northern to the Aspropyrgos fault at the southern base of the Fili mountain. Fig. 3cd shows the synthetic interferogram derived from model 2, as well as the mapped (F1 and F2) and modeled fault segments. A more detailed presentation commenting the fault parameters returned by models 1 and 2 with their associated uncertainty values is given in [7].

Table 1. Parameters describing the fault geometry and motion in the Okada formalism

Symbol	Description
Lat	Latitude of the center of the fault upper edge
Lon	Longitude of the center of the fault upper edge
α	Strike (°)
h	Depth of the upper edge of the fault (km)
d	Half-length of the fault (km)
L	Width of the fault (km)
θ	Dip angle (°)
S	Strike slip (positive left lateral) (mm)
D	Dip slip (positive normal) (mm)

Table 2. Fault parameters derived by model 2 (strike angle = 116°, dip angle = 54°, other parameters free)

Fault	Lat (°)	Lon (°)	h (km)	d (km)	L (km)	θ (°)	α (°)	S (mm)	D (mm)	M (Nm)
Main fault	38° 7' 33''	23° 35' 04''	5.9	5.2	11.0	54	116	50	350	12.1 10 ¹⁷
Secondary fault	38° 7' 23''	23° 41' 14''	4.0	4.5	3.5	54	116	35	260	2.5 10 ¹⁷

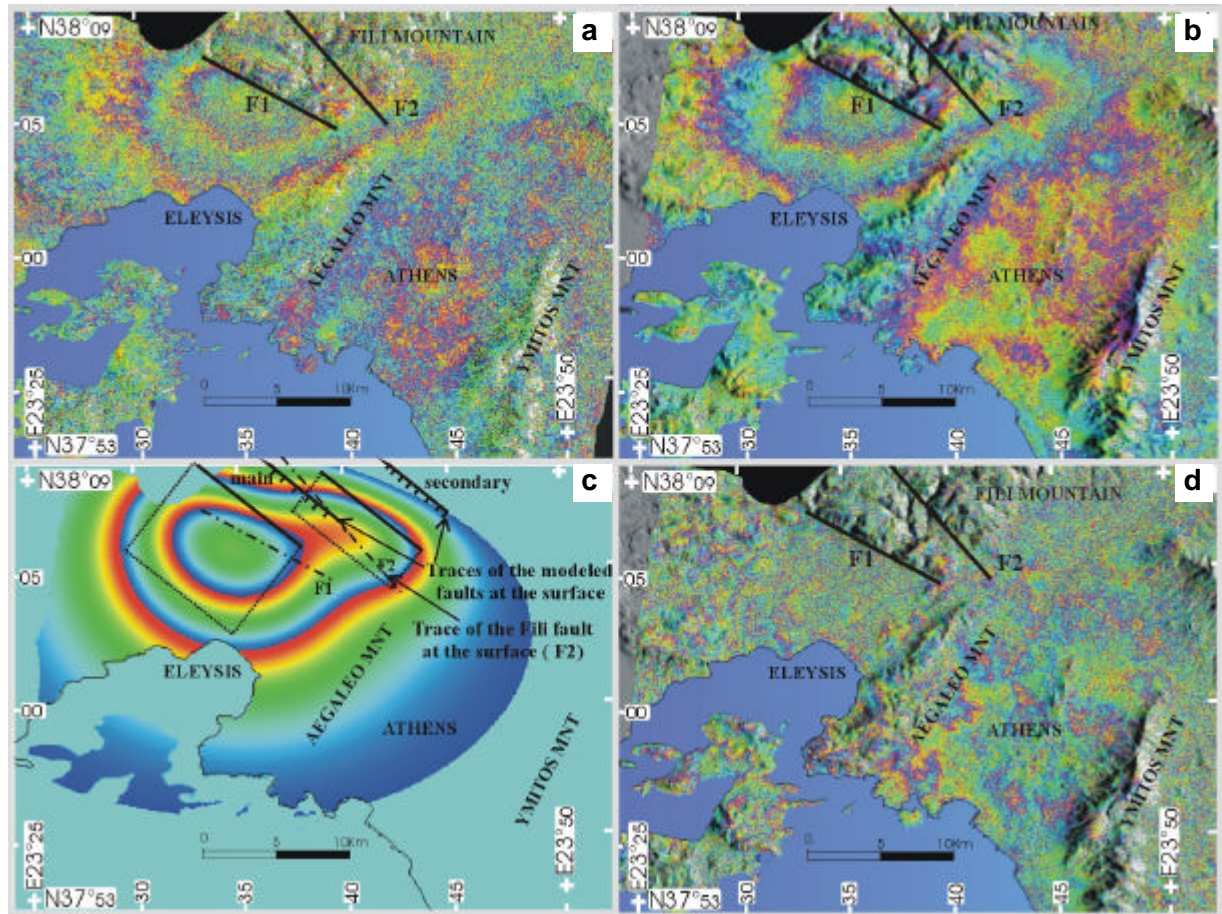


Fig. 3. (a, b) Coseismic interferograms spanning the periods [Nov. 27, 1997 to Sep. 23, 1999] and [Sep. 19, 1998 to Oct. 9, 1999]. (c) Modeled interferogram calculated by least square inversion of the fringes in Fig 3a and 3b. (d) Preseismic Interferogram spanning the period July 22, 1995 to July 15, 1999.

Conclusions

The co-seismic interferograms show that the affected area is extended for more than 20 km in the E-W and 10 km in the N-S directions and is bounded by the Fili mountain in the NE and the Aegaleo mountain in the SE (Plates 1c and 1d). The area defined by the fringes encompasses the vast majority of the located epicenters, extending SW to the Fili fault with a striking along a WNW-ESE axis. However, a high concentration of aftershocks is also observed at the eastern border of the Thriassion depression along the Aegaleo mountain, indicating most likely the activation of another zone related to the Aegaleo mountain. It should be noted however, that no fringes are observed beyond the root of the Aegaleo mountain, and this corroborates the opinion of other researchers that this mountain acted as a boundary, preventing further activation to the south-east direction (V. Papazachos, oral communication).

The absence of rupture propagation towards the Earth surface made difficult the direct identification of the seismogenic fault. According to our modeling study the main fault segment is located at the NW extension of the Fili fault as mapped by Pavlides in [17]. However, as we move towards the east, the modeled fault segment intersects the surface ~3 km northern to the Fili fault, which indicates that a secondary structure has been activated in this area (Fig. 3d). It is worth noting that the modeled faults do not appear on the existing geological and seismotectonic maps, suggesting the existence of a blind fault zone.

Case Study 2: The INSAR Signature of the Nisyros Volcano in Aegean Sea

Ground deformation by using ERS-2 SAR interferometry

Nisyros is part of the Aegean active volcanic island arc, situated at the eastern border. The island represents the emerged portion of an andesitic volcano [4], built up the last 100000 years [6], truncated by a summit caldera of 3.8 km of diameter formed as a consequence of intense explosive activity, less than 24000 y.B.P [6]. Post caldera activity was accomplished by intrusion of dacitic lava domes, along NE-trending tectonic system fractures, rising the caldera rim at a maximum height of 698 m [10]. Phreatomagmatic activity produced cones and craters a century ago. All the historically registered explosions are hydrothermal, with more than five phreatic explosions being reported since 1422 within the Nisyros caldera depression [22]. The occurrence of more than 8 older phreatic explosion craters in the caldera floor, indicate that this type of activity was frequent even before 1422. However, the last one reported occurred in 1888. The island is today a site of intensive hydrothermal activity, which feed many fumaroles in the caldera floor area and hot springs along the coastline. The risk of a phreatic explosion is high [19]. In such a case the human losses could be heavy since the island is being visited by thousands of tourists during the summer time.

At the end of 1995 an intense seismic activity manifested in the island lasting 3 years. A seismological operation was carried out on the island in order to investigate the factors controlling the seismic behavior of the Nisyros volcano. This recent long lasting episode of unrest in the area is of great importance and has attracted the interest of many scientists, because it is the first well instrumentally documented and could provide significant information on the behavioral model of the volcano. An operation using radar interferometry was initiated to measure the crust deformation associated with the volcano activity during the last years. The interferometric calculations have been based on the use of ERS-2 SAR images spanning the period from June 4, 1995 to September 10, 2000. From these interferograms it is demonstrated that a continuous vertical deformation of the surface of Nisyros island has occurred during this period. The satellite images were acquired at the ascending pass of the ERS-2 system, where the satellite travels approximately from south to north looking eastwards and inclined 23.5° from the vertical. As in the study of Athens earthquake the selection of the interferometric pairs to process was based on the altitude of ambiguity h_a parameter. Table 3 illustrates the time spanning of the interferometric pairs used and their corresponding h_a values.

The DEM was produced, as in the study of Athens earthquake, by digitizing contour lines and spot height data from existing 1:5000-scale topographic maps, achieving a height accuracy of the order of $\pm 10\text{m}$. As it may be resulted the magnitude of the expected topographic artifacts expressed in phase cycles, for the worst co-seismic pair ($h_a = 64\text{ m}$), would be of the order of 0.16 phase cycles or 4.375mm in range. The same calculation for the best co-seismic pair ($h_a = 180\text{m}$), yielded 0.055 cycles, that is equivalent to 1.55 mm in range.

Table 3. ERS-2 Image pairs used for interferometric calculations

Acq. Date Image No1	Acq. Date Image No 2	Altitude of Ambiguity h_a (m)	Satellite Orbits	Figure Code
4 June 1995	19 May 1996	99	641-5651	Fig. 4a
19 May 1996	8 June 1997	180	5651-11162	Fig. 4b
4 June 1995	8 June 1997	64	641-11162	Fig. 4c
8 June 1997	18 July 1999	120	11162-22184	-
24 May 1998	10 Sept. 2000	132	16172-28196	Fig. 4d-

This differential interferometry survey makes evident that crust deformations have occurred on the surface of Nisyros island during the years 1995-97, in which the most significant earthquake events have been recorded by the local seismograph array deployed. The calculated interferograms demonstrate a continuous surface uplift. The observed deformation field shows an approximately circular shape centered at the NW side of Nisyros island pointing to the area where the most intense seismic activity was recorded in March 1997 (Fig. 4a, 4b, 4c). In the interferogram spanning the period [June 4, 1995 to May 19, 1996] (Fig. 4a) three fringes are shown. They are semicircular (not closed) fringes due to the fact that the island surface is rather small and the deformed crust is extending beneath the sea surface. As a

consequence the surrounding sea interrupts the observed fringes. The fringes indicate a general uplift in the slant range direction of the order of 84 mm.

The following year (1996-97) the surface was displaced keeping the same trend. The two resulted fringes shown on the corresponding interferogram (Fig. 4b) [May 19, 1996 to June 8, 1997], indicate a further surface displacement of 56mm in range. It is worth noting that the magnitude of the deformation observed for the two year period [June 4, 1995 to June 8, 1997], as suggested by the corresponding interferogram (Fig. 4c), conforms well with the displacement magnitudes observed for the two sub-periods 1995-1996 and 1996-1997. Indeed as interferogram of Fig. 4c shows, the number of the resulted fringes equals the summation of the corresponding fringes on the interferograms of Fig. 4a and 4b respectively. It should be noted that according to the only existing study realized in Nisyros the year 1997 a general surface uplift trend has been reported [8]. This is the result of the study of a series of ground GPS observations conducted through the whole island during this year. From this interferometric analysis it becomes evident that the recent episode of Nisyros volcano unrest resulted, during the years 1995-1997, in crust deformations of the order of 140mm. The rate of change was rather higher in the period 1995-96 reaching an average value of 87mm/year. During the next year (1996-97) the same process of surface deformation is observed but the deformation rate tended to decrease by time to 53mm/year.

The study was not possible to extend in year 1998. This is because the only available in ESA's archives ERS-2 scene acquired on May 24, 1998 was not usable, due to the fact that all combinations with older images had inadequate h_a values, ranging between 12 m to 17 m, that is very close to the expected DEM error (± 10 m). Therefore it was not possible to identify the magnitude and the trend of the deformation during the year 1997-1998. The study continued for the years 1999-2000 and it was observed that the surface started moving towards the opposite direction as being the result of a deflation procedure that has started in the meantime. For this purpose new interferograms have been constructed by integrating two new images acquired on July 18, 1999 and September 10, 2000. The two interferograms spanning the periods [June 8, 1997 to July 18, 1999] and [May 24, 1998 to September 10, 2000] (Fig. 4d) show two and four fringes respectively, denoting a movement in the opposite direction of the one in interferograms calculated up to the year 1997 have suggested.

Assessing the deformation just by counting fringes in such a small area, which is obscured by sea and low coherence or shadowed and layover areas is rather difficult. For this reason, the current research is focussed on modeling the observed deformation field by fitting the interferograms with a calculated theoretical displacement field derived from a simple model of pressure change in a sphere located in an elastic half-space. These results will be subject of further analysis and publication.

Conclusions

Greek volcanoes are characterized by a paucity in recent eruptive and for this reason they are not permanently monitored. However, the study of the recorded earthquake activity in relation to the location and size of the ground vertical displacements help to understand about the presently active part of the volcanic caldera and the magmatic behavior of the volcano. Understanding the processes giving rise to episodes of unrest in a volcanic system greatly enhances the chances of correctly recognizing precursory signs to eruptions from that system.

The first results on the Nisyros study suggest that the presently active part of the Nisyros caldera appears to be much smaller than the known geological one with the existence of a magma chamber at the NW coast of Nisyros island. The inflation of this chamber is most likely responsible for the unrest episode, which was observed in 1995-1998 resulting to ground deformations (total uplift of 140mm) and also to intense seismic activity. The observed faulting in the island which has been the source of serious house damages is probably induced as a secondary effect of the vertical pressure increase (magma inflation) and is not the result of shear strain rise. No eruption followed this important unrest episode, in contrary to that of 1871-1873. However, one should take into consideration the case of the Rabaul caldera in Papua where the eruption took place 10 years after the last unrest episode [5]. This confirms the complexity of the volcano controlling mechanism and implies that monitoring activities especially at this part of the Hellenic Volcanic Arc are necessary not only during episodes of alarming activity but through the intervening apparent quiescent periods as well.

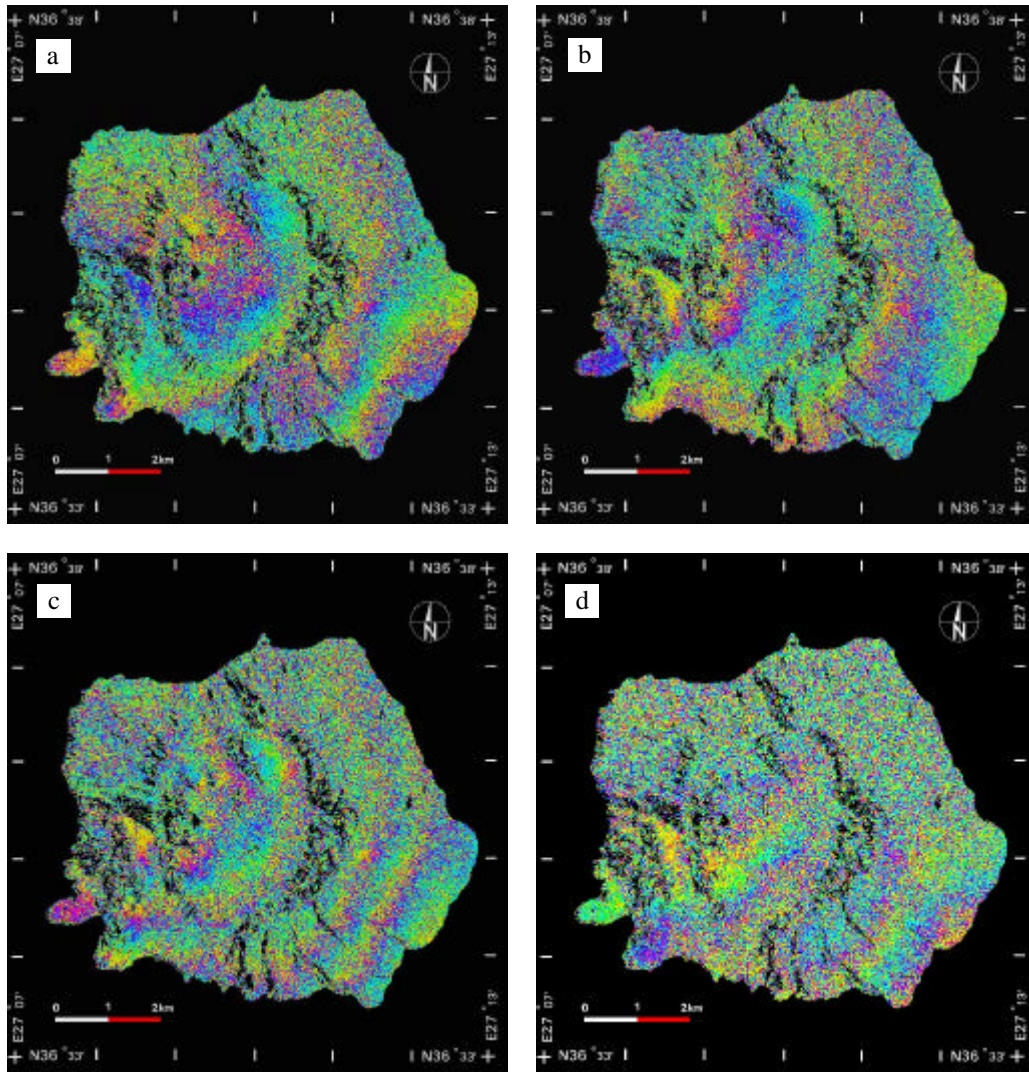


Fig. 4 Interferograms spanning the periods: (a) [June 4, 1995 to May 19, 1996], (b) [May 19, 1996 to June 8, 1997], (c) [June 4, 1995 to June 8, 1997], and (d) [May 24, 1998 to September 10, 2000]

ACKNOWLEDGEMENTS

The authors are grateful to the European Space Agency (ESA) for providing ERS-2 SAR data. Sincere thanks are due to Prof. N.N. Ambraseys for making available his internal field report on the Athens earthquake.

REFERENCES

- [1] A. Avallone, A. Zollo, P. Briole, C. Delacourt, and F. Beauducel, Subsidence of Campi Flegrei (Italy) detected by SAR interferometry, *Geophysical Research Letters*, Vol. 26, No 15, 2303-2306, 1999.

- [2] P. Bernard, et al., The Ms=6.2, June 15, 1995, Aigion earthquake (Greece): Evidence for low normal faulting in Corinth rift, *J. Seismology*, 1, 131-150, 1997.
- [3] Briole P., G. De Natale, R. Gaulon, F. Pingue and R. Scarpa, Inversion of geodetic data and seismicity associated with the Friuli earthquake sequence (1976-1977), *Annales Geophysicae*, 4, 481-492, 1986.
- [4] G. M. Di Paola, Volcanology and petrology of Nisyros Island (Dodecanese, Greece) *Bull. Volcanol.*, 38: 944-987, 1974.
- [5] O. Gudmundsson, R. W. Johnson, D. M. Finlayson, Y. Nishimura, H. Shimamura, A. Terashima, I. Itikarai, and C. Thurber, Multinational Seismic Investigation Focuses on Rabaul Volcano, *EOS, Trans. Am. Geophys. Un.*, 80-24: 272-273, 1999.
- [6] J. Keller, Th. Rehren, and E. Stadlbauer, Explosive Volcanism in the Hellenic Arc: a Summary and Review, *Proceedings of the third International Congress, Thera and the Aegean World III*, Volume Two 13-26, 1990.
- [7] C. Kontoes, P. Elias, O. Sykioti, P. Briole, D. Remy, M. Sachpazi, G. Veis, and I. Kotsis, Displacement field and fault model for the September 7, 1999 Athens earthquake inferred from ERS2 satellite radar interferometry, *Geophysical Research Letters*, in press.
- [8] E. Lagios, S. Chailas, I. Giannopoulos, and P. Sotiropoulos, Surveillance of the Nisyros volcano. Establishment and remeasurement of GPS and Radon networks. *Bull. Geol. Soc. Greece*, 32: 215-227 (in Greek with English abstr.), 1998.
- [9] Z. Lu, D. Mann, and Freymueller J., Satellite radar interferometry measures deformation of Okmok volcano, *EOS Transactions AGU*, Vol. 79, No 84, 464-469, 1998.
- [10] Marini L., Principe C., Chiodini G., Cioni R., Fytikas M., and Marinelli G., 1993. Hydrothermal eruptions of Nisyros (Dodecanese, Greece). Past events and present hazard *J. Volcanol. Geotherm. Res.*, 56: 71-94.
- [11] D. Massonnet, M. Rossi, C. Carmona, F. Adragna, G. Peltzer, K. Feigl, and T. Rabaute, The displacement field of the Landers earthquake mapped by radar interferometry, *Nature*, 364, 138-142, 1993.
- [12] D. Massonnet, P. Briole, and A. Arnaud, Deflation of mount Etna monitored by spaceborne radar interferometry, *Nature*, 375, 567-570, 1995.
- [13] D. Massonnet, and K. Feigl, Discrimination of geophysical phenomena in satellite radar interferograms, *Geophysical Research Letters*, Vol. 22, No 12, 1537-1540, 1995.
- [14] B. Meyer, R. Armijo, J. B. Chabalier, C. Delacourt, J. C. Ruegg, J. Acache, P. Briole, and D. Papanastassiou, The 1995 Greneva (Northern Greece) Earthquake: Fault model constrained with tectonic observations and SAR interferometry, *Geophysical Research Letters*, 23(19), 2, 677-2, 680, 1996.
- [15] M. Murakami, M. Tobita, S. Fujiwara, T. Saito, and H. Masaharu, Co-seismic crustal deformations of the 1994 Northridge, California, earthquake detected by interferometric JERS 1 Synthetic Aperture Radar, *Journal Geophysical Research*, 101, 8605-8614, 1996.
- [16] Y. Okada, Surface deformations due to shear and tensile faults in a half-space, *Bull. Seism. Soc. Am.*, 75, 1135-1154, 1985.
- [17] S. Pavlides, G.A. Papadopoulos, and A. Ganas, The 7th September, 1999 unexpected earthquake of Athens: Preliminary results on the seismotectonic environment, *paper presented at 1st Conf. Advances in Natural Hazards Mitigation: Experiences from Europe and Japan, Programme-Abstracts-Reports*, 80-85, 1999.
- [18] G. A. Papadopoulos, G. Drakatos, D. Papanastassiou, I. Kalogeras, and G. Stavrakakis, Preliminary results about the catastrophic earthquake of 7 September 1999 in Athens, Greece, *Seismological Research Letters*, 71, 3, 318-329, 2000.

- [19] St Seymour K, and D. Vlassopoulos, The potential for future explosive volcanism associated with dome growth at Nisyros, Aegean volcanic arc, Greece. *J. Volcanol. Geotherm. Res.*, 37: 351-364, 1989.
- [20] A. Tarantola, and B. Valette, Generalized nonlinear inverse problem solved using the least squares criterion, *Rev. Geophys. Space Phys*, 20, 219-232, 1982.
- [21] G. A. Tselentis, and J. Zahradnik, The Athens earthquake of September 7, 1999, *paper submitted to Bull. Seism. Soc. Am.* 1999.
- [22] G. Vougioukalakis, M. Sachpazi, K. Perissoratis, and Th. Liberopoulou, The 1995-1997 seismic crisis and ground deformation on Nisyros volcano, Greece: a volcanic unrest? Presentation on at the Sexta Reunion Internacional Volcan de Colima pp 2-18 Institute of Geology and Mineral Exploration, Unpublished Report, 1998.
- [23] H. A. Zebker, P.A. Rosen, R.M. Goldstein, A. Gabriel, and C.L. Werner, On the derivation of co-seismic displacement fields using differential radar interferometry: The Landers earthquake, *J. Geophys. Res.*, 99, 617-19,634, 1994.